Supporting Information for

Broadband generation of photonic spin-controlled arbitrary accelerating light beams in the visible

Qingbin Fan[1,2#], Wenqi Zhu[3,4,#], Yuzhang Liang[1,2#], Pengcheng Huo[1,2], Cheng Zhang[3,4], Amit Agrawal[3,4], Kun Huang[5], Xiangang Luo[6], Yanqing Lu[1,2], Chengwei Qiu[7,*], Henri J. Lezec[3,*] and Ting Xu[1, 2*]

1. *National Laboratory of Solid State Microstructures, College of Engineering and Applied Sciences and Collaborative Innovation Center of Advanced Microstructures, Nanjing University, Nanjing 210093, China*
2. *Key Laboratory of Intelligent Optical Sensing and Manipulation, Ministry of Education, Nanjing 210093, China.*
3. *Center for Nanoscale Science and Technology, National Institute of Standards and Technology, Gaithersburg, MD 20899, USA*
4. *Maryland NanoCenter, University of Maryland, College Park, MD 20742, USA.*
5. *University of Science and Technology of China, Hefei 230026, China*
6. *Institute of Optics and Electronics, Chinese Academy of Sciences, Chengdu 610209, China.*
7. *Department of Electrical and Computer Engineering, National University of Singapore,117583, Singapore*

# These authors contributed equally.

*Email: xuting@nju.edu.cn, henri.lezec@nist.gov, chengwei.qiu@nus.edu.sg

S1: Derivation of the Jones matrix J and its eigenvalues and eigenvectors.

Assuming input polarization states $\{|\alpha^+\rangle, |\alpha^-\rangle\}$ upon which the metasurface should impart two independent phase profiles, $\varphi_1(x,y)$ and $\varphi_2(x,y)$, be given by orthogonal polarization states $|\alpha^+\rangle = \begin{bmatrix}\alpha_1^+\\ \alpha_2^+\end{bmatrix}$ and $|\alpha^-\rangle = \begin{bmatrix}\alpha_1^-\\ \alpha_2^-\end{bmatrix}$. We can find a design of a linearly birefringent metasurface where the output polarization states become $\{|(\alpha^+)^*\rangle, |(\alpha^-)^*\rangle\}$; denoting complex conjugate of input polarization states. This means that they have the same states as the input states with flipped handedness. Such device can be described by Jones matrix $J(x,y)$ that simultaneously satisfies

$$J(x,y)\ \ |\alpha^+\rangle = e^{i\varphi_1(x,y)}|(\alpha^+)^*\rangle \tag{S1}$$

and

$$J(x,y)\ \ |\alpha^-\rangle = e^{i\varphi_2(x,y)}|(\alpha^-)^*\rangle \tag{S2}$$

In our design, the input polarization states are orthogonal circular polarizations states

$$|L\rangle = \begin{bmatrix}1\\ i\end{bmatrix} \tag{S3}$$

$$|R\rangle = \begin{bmatrix}1\\ -i\end{bmatrix} \tag{S4}$$

Then, the original system can be expressed as

$$J(x,y)\begin{bmatrix}1\\ i\end{bmatrix} = e^{i\varphi_1(x,y)}\begin{bmatrix}1\\ -i\end{bmatrix} \tag{S5}$$

and

$$J(x,y)\begin{bmatrix}1\\ -i\end{bmatrix} = e^{i\varphi_2(x,y)}\begin{bmatrix}1\\ i\end{bmatrix} \tag{S6}$$

Upon matrix inversion of Eq. S5 and S6, we obtain

$$J(x,y) = \begin{bmatrix} e^{i\varphi_1(x,y)} & e^{i\varphi_2(x,y)} \\ -ie^{i\varphi_1(x,y)} & ie^{i\varphi_2(x,y)} \end{bmatrix}\begin{bmatrix}1 & 1\\ i & -i\end{bmatrix}^{-1} \tag{S7}$$

Then, we can show that the desired matrix $J(x,y)$ is

$$J(x,y) = \frac{1}{2}\begin{bmatrix} e^{i\varphi_1(x,y)} + e^{i\varphi_2(x,y)} & ie^{i\varphi_2(x,y)} - ie^{i\varphi_1(x,y)} \\ ie^{i\varphi_2(x,y)} - ie^{i\varphi_1(x,y)} & -e^{i\varphi_1(x,y)} - e^{i\varphi_2(x,y)} \end{bmatrix} \tag{S8}$$

where $\varphi_1(x,y)$ and $\varphi_2(x,y)$ are phase profiles of arbitrary accelerating beams. This matrix provides a general form for conversion between two arbitrary accelerating beams and even arbitrary structured light. By calculating Jones matrix $J(x,y)$, we can obtain the eigenvalues as

$$\xi_1 = e^{i[\frac{1}{2}(\varphi_1(x,y)+\varphi_2(x,y))]} \qquad \xi_2 = e^{i[\frac{1}{2}(\varphi_1(x,y)+\varphi_2(x,y))-\pi]} \tag{S9}$$

and eigenvectors as

$$|r_1\rangle = \begin{bmatrix} \cos\frac{1}{4}[\varphi_1(x,y)-\varphi_2(x,y)] \\ sin\frac{1}{4}[\varphi_1(x,y)-\varphi_2(x,y)] \end{bmatrix} \qquad |r_2\rangle = \begin{bmatrix} -\sin\frac{1}{4}[\varphi_1(x,y)-\varphi_2(x,y)] \\ cos\frac{1}{4}[\varphi_1(x,y)-\varphi_2(x,y)] \end{bmatrix} \tag{S10}$$

Thus, the Jones matrix $J(x,y)$ can be decomposed into canonical form $J = P\Lambda P^{-1}$, where Λ is a diagonal matrix and P is an invertible matrix. We can write the Jones matrix for the control and conversion between two arbitrary optical beams as

$$J(x,y) = \mathrm{P}\Lambda\mathrm{P}^{-1} = \begin{bmatrix} \cos\frac{1}{4}[\varphi_1(x,y)-\varphi_2(x,y)] & -\sin\frac{1}{4}[\varphi_1(x,y)-\varphi_2(x,y)] \\ sin\frac{1}{4}[\varphi_1(x,y)-\varphi_2(x,y)] & cos\frac{1}{4}[\varphi_1(x,y)-\varphi_2(x,y)] \end{bmatrix}\cdots$$

$$\begin{bmatrix} e^{i[\frac{1}{2}(\varphi_1(x,y)+\varphi_2(x,y))]} & 0 \\ 0 & e^{i[\frac{1}{2}(\varphi_1(x,y)+\varphi_2(x,y))-\pi]} \end{bmatrix} \begin{bmatrix} \cos\frac{1}{4}[\varphi_1(x,y)-\varphi_2(x,y)] & -\sin\frac{1}{4}[\varphi_1(x,y)-\varphi_2(x,y)] \\ sin\frac{1}{4}[\varphi_1(x,y)-\varphi_2(x,y)] & cos\frac{1}{4}[\varphi_1(x,y)-\varphi_2(x,y)] \end{bmatrix} \tag{S11}$$

Since Jones matrix $J(x,y)$ works in the linear polarization basis and P can be regarded as a rotation matrix for the matrix Λ, we can obtain that the phase shifts are $\delta_x(x,y) = [\varphi_1(x,y) + \varphi_2(x,y)]/2$ and $\delta_y(x,y) = [\varphi_1(x,y) + \varphi_2(x,y)]/2 - \pi$ and the rotation angle is $\theta(x,y) = [\varphi_1(x,y) - \varphi_2(x,y)]/4$.

S2: Calculation of polarization conversion efficiency

The unit cell is simulated by using finite-difference time-domain (FDTD) method. In the simulation, a linearly polarized plane wave $|E_{in}\rangle$ is normally incident onto a single nanopost from substrate with periodic boundary conditions. The spectra of transmission coefficients t_x and t_y were obtained from the simulation. The phase difference between the transmission coefficients t_x and t_y is denoted by φ. The polarization conversion efficiency η_R (from LCP to RCP) and η_L (from RCP to LCP) can be calculated by following equations [1]:

$$\eta_R = \left|\frac{1}{2}(t_x - t_y e^{i\varphi})\langle L|E_{in}\rangle\right|^2$$

$$\eta_L = \left|\frac{1}{2}(t_x - t_y e^{i\varphi})\langle R|E_{in}\rangle\right|^2$$

Here, $\langle L|E_{in}\rangle$ denotes an inner-product of left-circularly polarized unit vectors and incident plane wave. Similarly, $\langle R|E_{in}\rangle$ denotes an inner-product of right-circularly polarized unit vectors and incident plane wave.

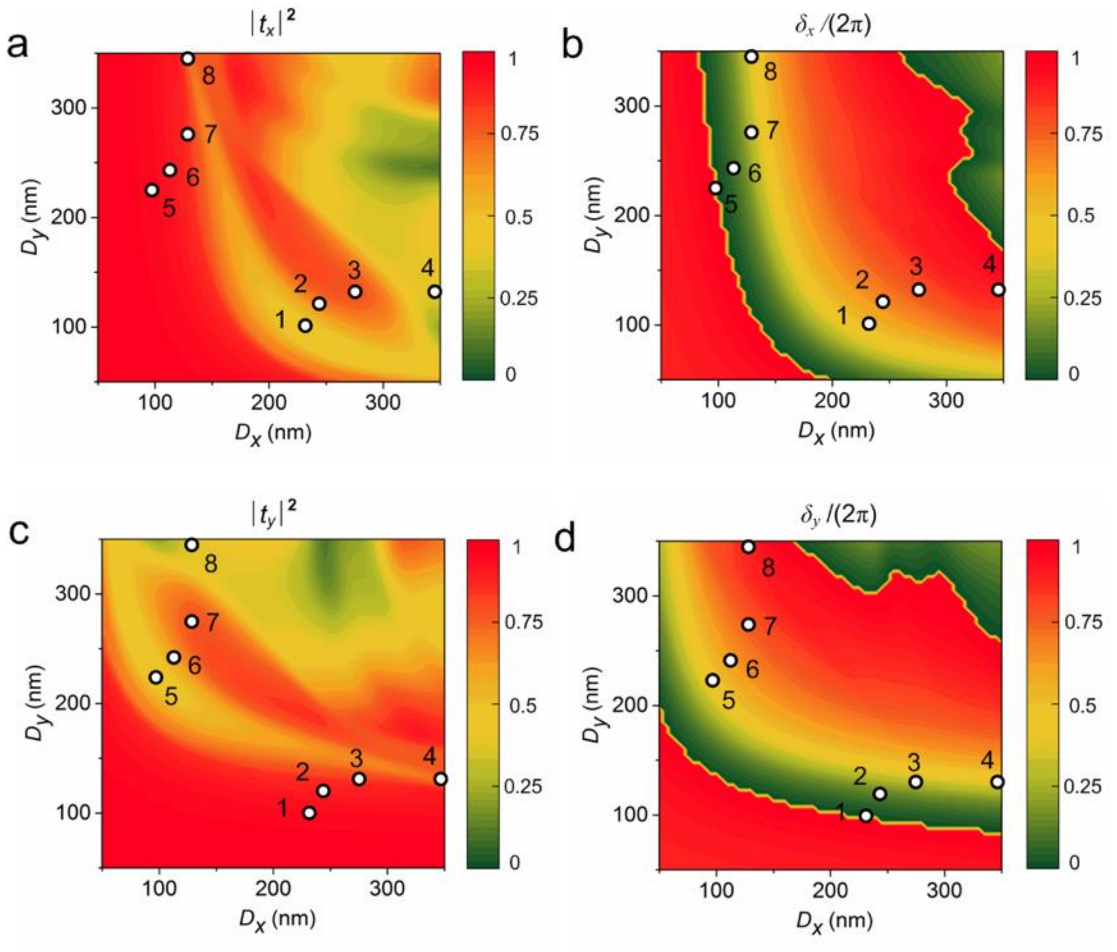

Figure S1. Calculated intensity transmission coefficients (a. $|t_x|^2$; c. $|t_y|^2$) and phase shifts (b. δ_x; d. δ_y) of transmission coefficients as a function of elliptical nanopost diameters (D_x, D_y) at the wavelength of 532 nm. The white dots indicate four fundamental nanopost structures nanopost #1-#4. The other four mirror structures #5 ~ #8 can be obtained just by switching D_x and D_y on nanopost #1-#4.

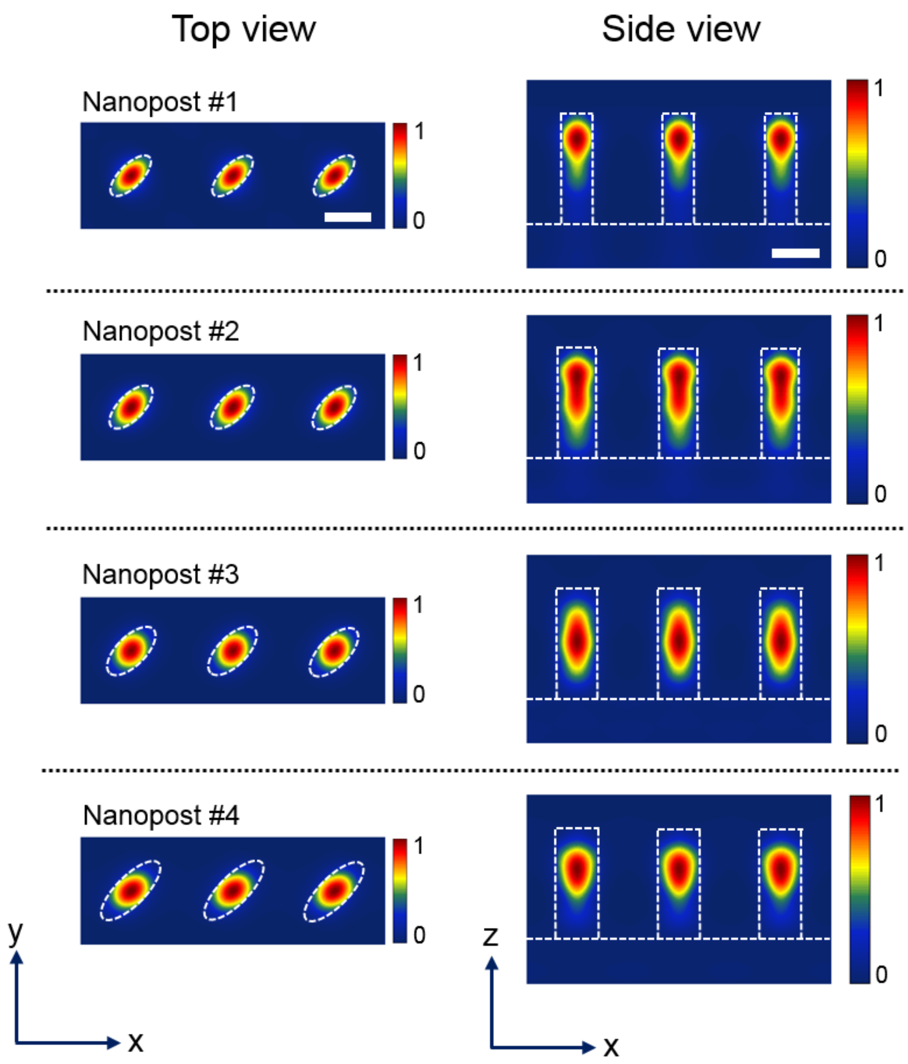

Figure S2. Top views (left: *xy* cross-section) and side views (right: *xz* cross-section) of the normalized energy density in a periodic array for different nanopost structures. The array of nanoposts are rotated by 45° with respect to the square lattice. A plane wave with *y*-polarization is normally incident on the TiO_2 nanoposts from the substrate side. The boundaries of the nanoposts are depicted by dashed white lines. Scale bars represent 200 nm in all figures.

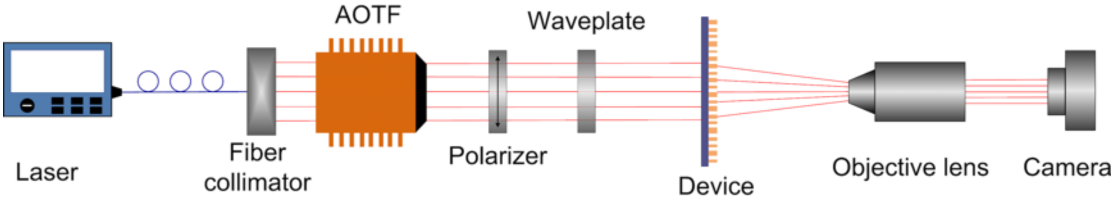

Figure S3. Schematic illustration of the measurement setup used for characterization of metasurface devices generating switchable accelerating light beams. The quarter-wave plate (QWP) is rotated to convert the polarization of incident light from LCP to RCP. AOTF: Acousto-Optic Tunable Filter system.

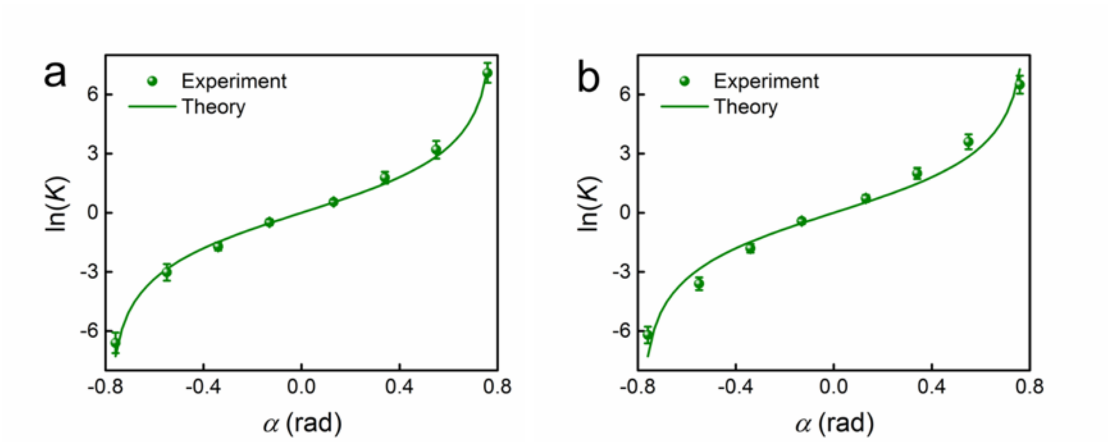

Figure S4. Calculated and measured intensity ratio K (in logarithmic scale) between $|R\rangle|A_l\rangle$ and $|L\rangle|A_r\rangle$ as a function of the QWP rotation angle α for the metasurface devices generating (a) two Airy beams and (b) biquadratic and natural logarithm beams. The uncertainties are standard deviation of intensity ratio for repeated experimental measurements (four in total).

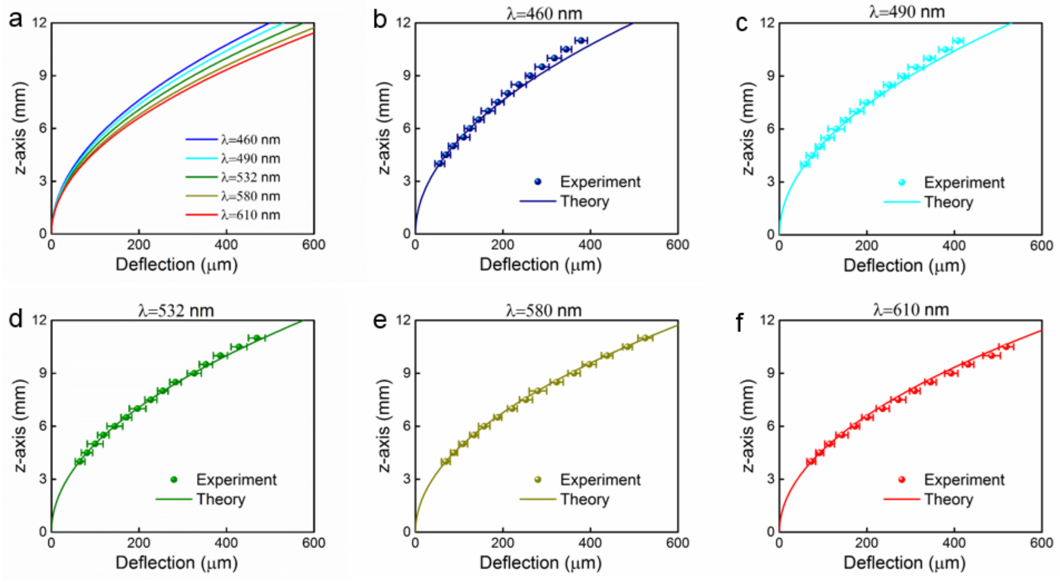

Figure S5. (a) Calculated propagation trajectories of the metasurface-generated Airy beams under the illumination at different wavelengths. (b)-(f) Experimentally measured propagation trajectories of Airy beams at different wavelengths. The uncertainties are standard deviation of deflection distance for repeated experimental measurements (four in total).

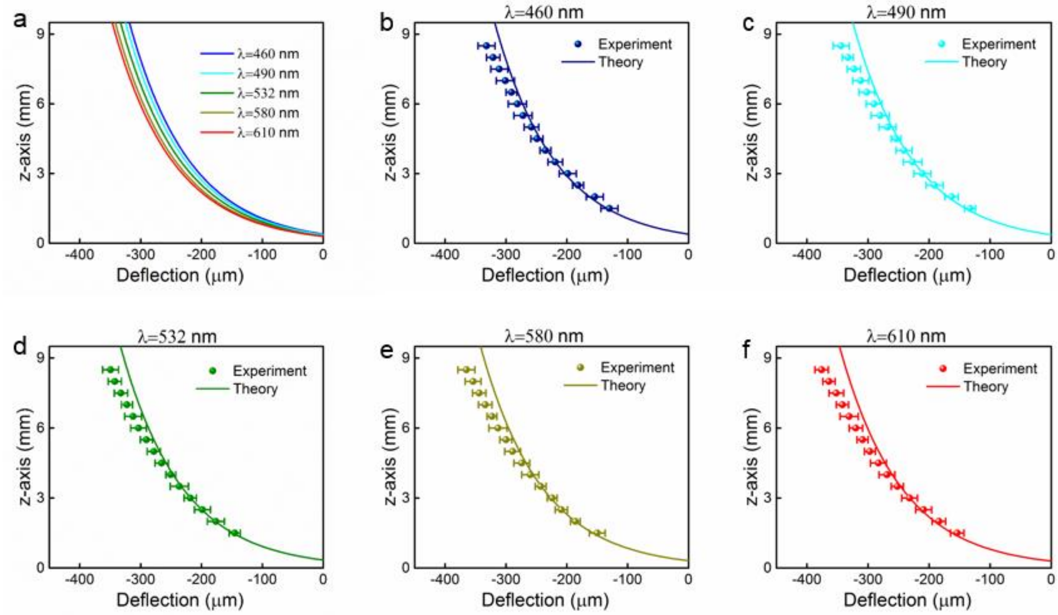

Figure S6. (a) Calculated propagation trajectories of the metasurface-generated accelerating beam following natural logarithm caustic trajectories under the illumination at different wavelengths. (b)-(f) Experimentally measured propagation trajectories of accelerating beams at different wavelengths. The uncertainties are standard deviation of deflection distance for repeated experimental measurements (four in total).

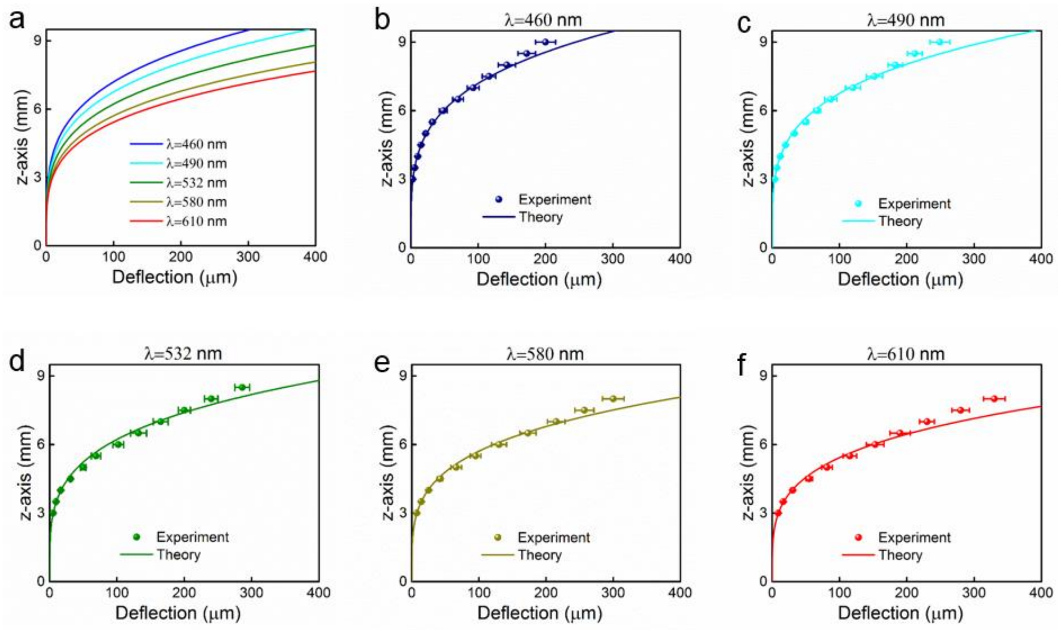

Figure S7. (a) Calculated propagation trajectories of the metasurface-generated accelerating beam following biquadratic caustic trajectories under the illumination at different wavelengths. (b)-(f) Experimentally measured propagation trajectories of accelerating beams at different wavelengths. The uncertainties are standard deviation of deflection distance for repeated experimental measurements (four in total).

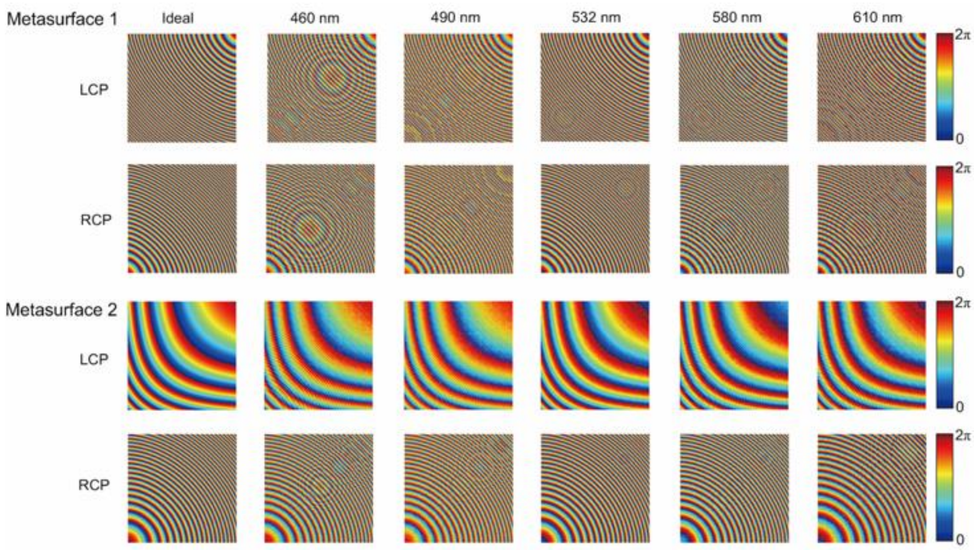

Figure S8. The calculated phase profiles of two metasurfaces for LCP and RCP light at multiple wavelengths. For ease of clear visualization, here we only plot phase profiles of a quarter of the metasurface area. As shown in these figures, the phase profiles of these two TiO_2 metasurfaces are very similar for the selected multi-wavelengths.

Table S1. The generation efficiencies of two metasurfaces for ALBs at different wavelengths.

Metasurface	460 nm	490 nm	532 nm	580 nm	610 nm
Metasurface 1 Airy beam	34%	46%	56%	48%	41%
Metasurface 2 $C_1(z)=a\ln(bz)$	36%	53%	61%	54%	46%
Metasurface 2 $C_2(z)=cz^4$	31%	51%	53%	40%	32%

References

[1] Lin, D., Fan, P., Hasman, E. & Brongersma, M. L. *Science* **2014**, 345, 298–302.